The Journal of Neuroscience, November 1993, 13(11): 4936–4948

Low-Threshold Ca^{2+} Current and Its Role in Spontaneous Elevations of Intracellular Ca^{2+} in Developing *Xenopus* Neurons

Xiaonan Gu and Nicholas C. Spitzer

Department of Biology and Center for Molecular Genetics, University of California at San Diego, La Jolla, California 92093

Amphibian spinal neurons exhibit spontaneous elevations of intracellular calcium at early stages of development. The underlying calcium influx involves high-voltage-activated (HVA) currents. To begin to understand how they are triggered, we have studied the biophysical properties and developmental function of low-voltage-activated (LVA) T-type calcium current of neurons cultured from the embryonic neural plate. T current was recorded from young neurons (6–9 hr *in vitro*) and from mature neurons (18–48 hr *in vitro*) using whole-cell voltage clamp. For both young and mature neurons, T current has a low threshold and is activated at membrane potentials positive to −60 mV in 2 mM extracellular calcium. The current is maximal at −35 mV with a mean peak amplitude of ~50 pA. Nickel blocks both LVA and HVA currents, but the former are 20-fold more sensitive. Amiloride also blocks T current selectively. T current is recorded in 87% of young neurons. This percentage drops to 67% in mature neurons after 1 d in culture and to 35% in mature neurons after 2 d in culture. There are no significant developmental changes in T current threshold, peak density, time course of activation and inactivation, and pharmacological sensitivity to blockers from 6 to 48 hr in culture.

Spontaneous transient calcium elevations in young neurons assayed by fluo-3 fluorescence are blocked by nickel or amiloride at concentrations that specifically block T current. T current has the lowest threshold among other inward currents in young neurons. Moreover, mathematical simulations show that T current lowers the threshold of the action potential by 15 mV. We conclude that T current can depolarize cells and trigger action potentials, and constitutes part of the cascade of events leading to spontaneous elevations of intracellular calcium in cultured neurons at early stages of differentiation.

[Key words: calcium T current, calcium high-voltage-activated currents, development, neuronal differentiation, spontaneous calcium influx, spinal cord,* Xenopus *embryos, whole-cell recording]

Many studies have shown that calcium plays important roles in development of nervous systems. Intracellularly, it mediates various calcium-dependent events. Calcium may be elevated by influx through membrane channels and by release from intracellular stores (Lipscombe et al., 1988; Tsien and Tsien, 1990; Meyer and Stryer, 1991). During early development of embryonic amphibian spinal neurons and differentiation of rat pheochromocytoma cells, changes in levels of intracellular calcium ($[Ca^{2+}]_i$) occur by both mechanisms (Holliday and Spitzer, 1990; Holliday et al., 1991; Reber and Reuter, 1991).

Voltage-dependent calcium channels are well-known pathways for calcium influx. Based on their thresholds of activation, channels have been classified as high-voltage activated (HVA) and low-voltage activated (LVA) (Tsien et al., 1988; Beam, 1989; Hess, 1990; Swandulla et al., 1991). Both types of calcium channels have been found in a variety of excitable cells (Fox et al., 1987a,b; Tsien et al., 1987; Beam, 1989; Hess, 1990), including embryonic neurons (Carbone and Lux, 1984; Gottmann et al., 1988; Kostyuk et al., 1988; McCobb et al., 1989; Barish, 1991a; Gu and Spitzer, 1991; Desarmenien et al., 1993). In *Xenopus* embryonic neurons HVA calcium current is present at early stages of development (Barish, 1986; O'Dowd et al., 1988). This current promotes calcium influx during long-duration calcium-dependent action potentials in these cells (Spitzer and Lamborghini, 1976; Baccaglini and Spitzer, 1977; Barish, 1991b; Lockery and Spitzer, 1992).

Embryonic *Xenopus* spinal neurons go through a calcium-sensitive period during their early development in culture. Removal of extracellular calcium during this period alters morphological differentiation, synapse formation, neurotransmitter phenotype, and ion channel function (Bixby and Spitzer, 1984; Henderson et al., 1984; Holliday and Spitzer, 1990; Desarmenien and Spitzer, 1991; Spitzer et al., 1993). Spontaneous elevations of $[Ca^{2+}]_i$ are observed during this period using the indicator fura-2 AM (Holliday and Spitzer, 1990), and these elevations are blocked by removal of extracellular calcium or by blockade of HVA calcium current. These results suggest that influx through HVA calcium channels mediates the changes in intracellular concentrations during the calcium-sensitive period. The increase in $[Ca^{2+}]_i$ is due largely to release from intracellular stores, stimulated by influx of calcium (Barish, 1991b; Holliday et al., 1991).

We address specifically the mechanism by which spontaneous calcium influx is triggered in young neurons, leading to calcium release and increase of intracellular free calcium during the calcium-sensitive period. LVA calcium T current has been recorded in *Xenopus* spinal neurons at 1 d in culture (Barish, 1991a), when they are mature in many respects. Activation of T current by depolarization with potassium ions yields a slight increase in $[Ca^{2+}]_i$. Here we show that the current is already present during the earlier calcium-sensitive period and char-

Received Feb. 3, 1993; revised May 21, 1993; accepted May 27, 1993.

We thank Steve Watt for technical support, and Beverly Clendening, Devorah Gurantz, and Shawn Lockery for comments on the manuscript. This work was supported by NIH NS15918.

Correspondence should be addressed to Nicholas C. Spitzer, Department of Biology, 0322, UCSD, 9500 Gilman Drive, La Jolla, CA 92093-0322.

acterize its changes during development. We find several lines of evidence to indicate that T current plays a significant role in stimulating substantial elevations of $[Ca^{2+}]_i$ by triggering depolarization of neurons and activating HVA calcium current to promote influx during early development. This function is subsequently eliminated with further neuronal maturation.

Materials and Methods

Cultures. Cultures were prepared from embryos of *Xenopus laevis* obtained by standard breeding procedures. Developmental stages were assessed according to the criteria of Nieuwkoop and Faber (1967). Cultures were established as described in previous studies (Spitzer and Lamborghini, 1976; Ribera and Spitzer, 1989; Holliday and Spitzer, 1990; Desarmenien and Spitzer, 1991). (1) Mixed cultures used for whole-cell recordings contained neurons and myocytes in conjunction with other cell types. Tissue from the posterior presumptive spinal cord region of stage 15 (neural plate) embryos was dissected and then dissociated in divalent cation–free medium (in mM: 116.7 NaCl, 0.67 KCl, 0.4 EDTA, and 4.6 Tris with pH adjusted to 7.8 with HCl). Cultures were plated on 35 mm tissue culture dishes (Falcon or Costar). Culture medium contained (in mM) 116.7 NaCl, 0.67 KCl, 1.31 $MgSO_4$, 10 $CaCl_2$, and 4.6 Tris; pH was adjusted to 7.8 with HCl. (2) Neuron-enriched cultures used for calcium imaging experiments contained neurons and non-neuronal cells but were essentially free of myocytes. The same dissected tissue was treated with collagenase B (1 mg/ml; Sigma) in low-calcium medium (in mM: 58.8 NaCl, 0.67 KCl, 0.5 $CaCl_2$, and 8 HEPES, pH adjusted to 7.8 with NaOH) for 5–15 min. Following this treatment, the ectoderm, which includes the neural folds, was separated from mesoderm, endoderm, and notochord, and dissociated in divalent cation–free medium with 58.5 mM NaCl. Cultures were plated in medium containing (in mM) 58.8 NaCl, 0.67 KCl, 1.31 $MgSO_4$, 10 $CaCl_2$, and 4.6 Tris; pH was adjusted to 7.8 with HCl. In calcium imaging experiments, 58.8 mM NaCl medium was used in neuron-enriched cultures to facilitate comparison with previous experimental results (Holliday and Spitzer, 1990; Holliday et al., 1991), in which this NaCl concentration was used. In control experiments, calcium currents recorded from cells grown in this concentration (enriched cultures) showed no difference from those of cells grown in the higher concentration (mixed cultures). Cultures examined at 6–9 hr *in vitro* are referred to as young, while those examined at 18–48 hr *in vitro* are referred to as mature, reflecting the extent of differentiation of ion channels (O'Dowd et al., 1988; Ribera and Spitzer, 1990).

Recording conditions and solutions. Recording procedures were similar to those previously described (O'Dowd et al., 1988; Desarmenien and Spitzer, 1991). Cultured neurons were viewed on a Zeiss microscope using 10× oculars and a 40× water immersion objective lens with phase-contrast optics (Ph2, 0.75 NA). Conventional whole-cell voltage-clamp techniques were used to study calcium currents (Hamill et al., 1981). Pipettes were filled with intracellular recording solution and had 2–5 MΩ resistance in extracellular recording solution. Currents were recorded with an Axopatch-1D amplifier with a CV-4 headstage (1 GΩ; Axon Instruments, Inc.), filtered at 2 kHz, and digitized with a TL-1 DMA interface at sampling intervals from 40 to 100 μsec (Axon Instruments, Inc.). Inward currents greater than 5 pA were detectable in most cells. The threshold of a current was based on its voltage of activation. Data were acquired and stored with pCLAMP software (Axon Instruments, Inc.) and a DTK PC-compatible computer.

The pipette solution contained (in mM) 90 CsCl, 10 EGTA, 10 tetraethylammonium (TEA)-Cl, and 10 HEPES. An additional 2 mM concentration of ATP-Mg^{2+} and cAMP were added to this solution immediately prior to use and the pH was adjusted to 7.4 with CsOH. The presence of nucleotides prevented rundown of HVA calcium current but had no effect on LVA T current. CsCl was replaced with CsF when F^- was applied intracellularly to block HVA calcium currents. Extracellular recording solution contained (in mM) 80 NaCl, 40 TEA-Cl, 2 $CaCl_2$, 3 KCl, 5 HEPES, and 1 μg/ml tetrodotoxin (TTX); pH was adjusted to 7.4 with NaOH. The calcium dependence of currents was tested by equimolar replacement of $CaCl_2$ with $MgCl_2$, for which the channels have no significant permeability, and addition of 10 mM EGTA. In pharmacological studies, reagents used to block T current were applied by perfusion or direct addition to the recording solution. When sodium current was recorded, 2 mM external $CaCl_2$ was replaced by 2 mM $CoCl_2$ and TTX was omitted.

Data analysis. pCLAMP software was used for most data analysis. Currents were averaged from one to five trials, and peak currents were normalized to membrane surface area that was estimated from membrane capacitance (1 pF ≈ 0.01 μm^2; O'Dowd et al., 1988). The time course of activation was measured as the time from stimulus onset to half-maximum current ($t_{1/2}$) at different step potentials (V_S). The rate of inactivation was examined by fitting a single exponential to the decaying part of the current after the peak.

Activation was expressed as the fraction of maximum conductance ($V_S = -35$ mV). T current amplitudes at different membrane potentials were transformed into conductances (G) according to the equation $G = I/(V - E_{Ca})$. The reversal potential (E_{Ca}) for calcium current was estimated by extrapolation of the current–voltage relation (Fig. 1). Steady-state inactivation of T current was studied by systematically changing the holding potential (V_H) in depolarizing steps. Cells were held at each potential for 30 sec, and then depolarized to a test potential of −35 mV for 120 msec. Currents recorded at different holding potentials were normalized to maximum T current, recorded from $V_H = -110$ mV, to obtain the fraction of the current remaining at each holding potential. Dose–response curves for pharmacological inhibitors were fit by sigmoid relations with SIGMAPLOT software (Jandel Corp.). All averaged data are presented as mean ± SEM for the number of neurons indicated in parentheses. Student's t test was used to evaluate the significance of differences between mean values.

Computer simulation. T current was modeled with simplified Hodgkin-Huxley equations. A single family of LVA calcium T currents, obtained by depolarization to a series of step potentials, was chosen to illustrate the mean current–voltage relation and kinetics of activation and inactivation. Parameters specifying steady-state activation and inactivation and time constants for each were chosen as previously described in modeling high-voltage-activated currents (Lockery and Spitzer, 1992). Calcium dynamics were defined by a compartmental model in which intracellular submembrane calcium is supplied by calcium currents and removed by diffusion to an interior compartment. The effects of addition of T current on activation of calcium-dependent potassium current (I_{K_C}) and on the threshold of action potential initiation were evaluated as in previous simulations (Lockery and Spitzer, 1992). The threshold for production of the action potential was assessed from the voltage at which it could be initiated.

Action potentials were simulated under conditions of 10 mM external calcium to be comparable with previous intracellular recordings. The I–V relation of T and HVA current is shifted by +15 mV, as extracellular calcium is increased from 2 to 10 mM (data not shown). The voltage of activation of T current was thus shifted to the right by 15 mV, to reflect the effect on surface charge due to the increase in external calcium concentration from 2 mM (recordings) to 10 mM (simulations; Lockery and Spitzer, 1992), and the membrane permeability was increased. These changes yielded a simulated current with an I–V relation and kinetics similar to those recorded in 10 mM external calcium. The voltage of activation of I_{K_C} was shifted to the right by 10 mV, to reflect the difference in surface charge between recording (0.1 mM Ca^{2+}, 5 mM Mg^{2+}) and simulation conditions. Other currents were recorded under conditions ionically equivalent to 10 mM Ca^{2+}, and no surface charge adjustment was made for simulations.

Fluorescence image analysis. Changes in fluorescence of the calcium indicator fluo-3 AM (Minta et al., 1989) were used to study the function of LVA T current in triggering elevation of $[Ca^{2+}]_i$ during the calcium-sensitive period. Loading of dye and examination of "active" cells, which exhibited elevation of $[Ca^{2+}]_i$ during a 100 sec test period, were similar to those described previously (Holliday and Spitzer, 1990; Holliday et al., 1991). In short, the dye was first dissolved in dimethyl sulfoxide (50 μg/10 ml) and added to culture dishes at 6–9 hr *in vitro* to achieve a final concentration of 1–2 μM. After incubation for 30 min, cells were washed three times in culture medium over a period of 30 min or more. Dye-loaded cells were visualized on a Zeiss Photoscope with a 16× Neofluor objective. Fluo-3 fluorescence with emission at 520–540 nm was elicited using a 100 W DC mercury lamp and 490 nm excitation filter. Fluorescent images were obtained with an SIT camera (SIT 68, MTI) and a Hamamatsu Photonics image processing system (C1966) with a resolution of 640 × 483 × 16 bits. For examination of active cells, two fluorescent images of the same field were accumulated during two consecutive 100 sec periods. The first image was used as a background and subtracted from the second one, used as a test image. Only those cells exhibiting elevation of $[Ca^{2+}]_i$ during the 100 sec test period remained after subtraction; images from other cells canceled out

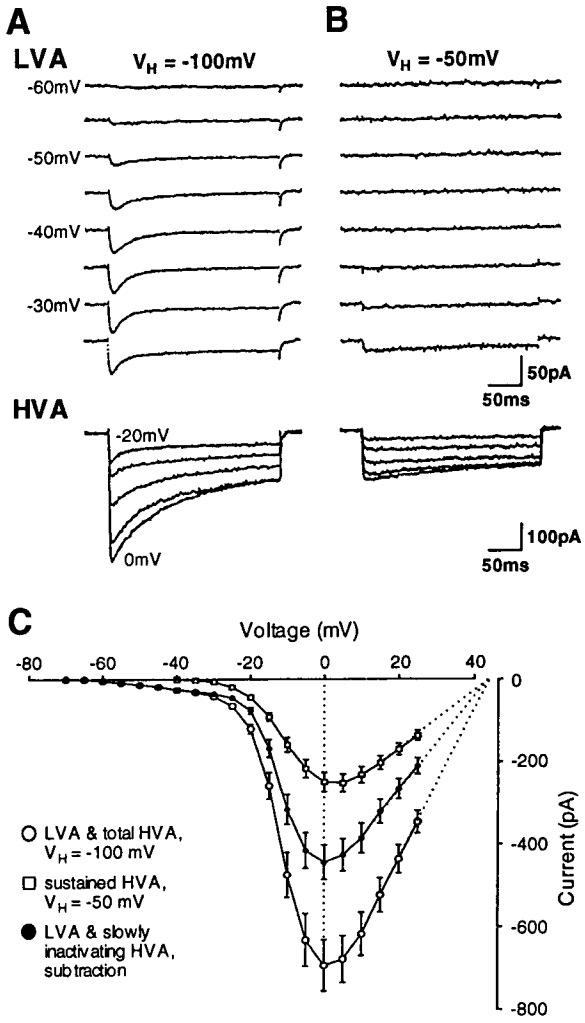

Figure 1. LVA (T) and HVA calcium currents in cultured *Xenopus* embryonic spinal neurons: records from a mature neuron depolarized from −60 to 0 mV (V_S) in 5 mV steps. *A*, At holding potentials (V_H) of −100 mV, LVA T-type current (*top*) is activated at membrane potentials positive to −60 mV and rapidly inactivated. It is the predominant inward current at step potentials of −60 to −30 mV. HVA currents (*bottom*) are activated at membrane potentials positive to −35 mV and are slowly inactivating. *B*, At V_H = −50 mV, T current is completely inactivated (*top*). Slowly inactivating HVA current is also eliminated, and only relatively steady HVA current remains (*top* and *bottom*). Rates of inactivation: τ_i (slowly inactivating, 0 mV), 66 msec (*A*); τ_i (relatively steady, 0 mV), 166 msec (*B*). *C*, Current–voltage relationships for both LVA (T) and HVA currents. *Open circles*, V_H = −100 mV. T current is seen at step potentials from −60 to −40 mV, and is then mixed with and masked by HVA currents. *Squares*, V_H = −50 mV. The relatively steady component of HVA current persists, and the rapidly inactivating T current and slowly inactivating component of HVA current are eliminated. *Solid circles*, T and slowly inactivating components are revealed by subtracting the current elicited with V_H = −50 mV from the current with V_H = −100 mV. Peak values of HVA currents occur near 0 mV for both holding potentials. Data are mean ± SEM of 28 mature cells.

each other. This image analysis was used to determine the percentage of active cells with and without blockade of T current. The quenching of indicator fluorescence by divalent cations is a potential concern (e.g., Ni^{2+}; Alonso et al., 1990). However, Ni^{2+} has been reported to have no effect on fluorescence at the concentrations we used (Murray and Kotlikoff, 1991). Furthermore, no change in baseline fluorescence intensity was detected following application of 50 μM nickel. Each imaged field usually contained 20–80 cells and several fields were examined in each culture for each experimental condition. Live image signals from

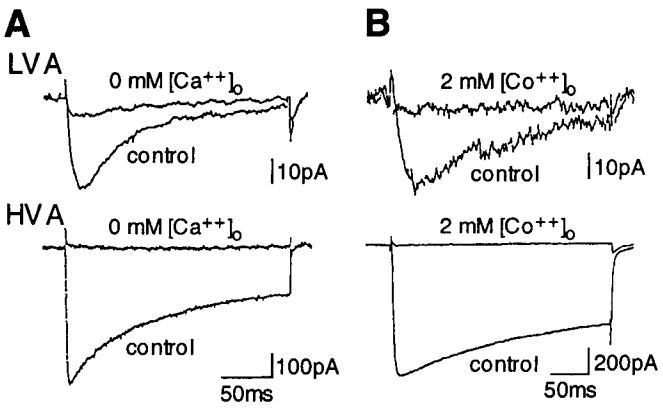

Figure 2. Removal of calcium or addition of cobalt eliminates LVA (T) and HVA currents. *A*, Removal of $CaCl_2$ from the bath solution and replacement with $MgCl_2$ eliminates both currents. Small residual currents may be due to Na^+ flux through these channels in the absence of Ca^{2+} (see text below). *B*, $CoCl_2$ (2 mM) blocks both the LVA and HVA currents. Records are from two mature neurons at 1 d in culture. *LVA*: V_H = −100 mV, V_S = −35 mV; *HVA*: V_H = −100 mV, V_S = 0 mV.

the SIT video camera were sent to a VCR as well as to the image processing system. The time course of changes in $[Ca^{2+}]_i$ in active cells was later analyzed by replay from the tape, using a QuickCapture frame grabber board (Data Translation) and the IMAGE program (W. Rasband, NIH); fluorescence intensities were digitized at 3 sec intervals.

Results

Voltage-activated calcium currents in Xenopus *embryonic spinal neurons*

Several ionic currents have been described in *Xenopus* embryonic spinal neurons, including HVA and LVA calcium currents, sodium current, several types of potassium currents, and calcium-dependent chloride current (Barish, 1986, 1991a; Harris et al., 1988; O'Dowd et al., 1988; Ribera and Spitzer, 1990; Hussy, 1991). In the present study, we have used whole-cell voltage clamp to analyze calcium currents in both young and mature neurons cultured from the *Xenopus* neural plate. We have focused on the LVA T-type calcium current and its role in regulating $[Ca^{2+}]_i$ in young neurons. In addition, we have further characterized the HVA current and find that it includes two components, a slowly inactivating current and a sustained current.

LVA calcium current. LVA currents were elicited from young and mature neurons when membrane potentials of cells were held at −100 mV and stepped to various depolarized potentials for 80–240 msec. Sodium currents were blocked by TTX and potassium currents were suppressed by a combination of intracellular CsCl and TEA-Cl plus extracellular TEA-Cl. T current was first activated when cells were depolarized above −60 mV; in most cells (n > 200) its threshold lay between −60 and −50 mV (Fig. 1*A*, top). With V_H = −100 mV, LVA current defines the current–voltage relation for step potentials below −40 mV (Fig. 1*C*, circles). The current was generally less than 100 pA in amplitude. It was transient, inactivating rapidly, and disappeared completely when V_H was shifted to −50 mV (Fig. 1*B*, top).

Replacement of extracellular calcium with magnesium eliminated this current (Fig. 2*A*, top). Cobalt (2 mM) also blocked LVA current in the presence of calcium (Fig. 2*B*, top). When extracellular calcium was removed, sodium became the major charge carrier for LVA current in the absence of magnesium

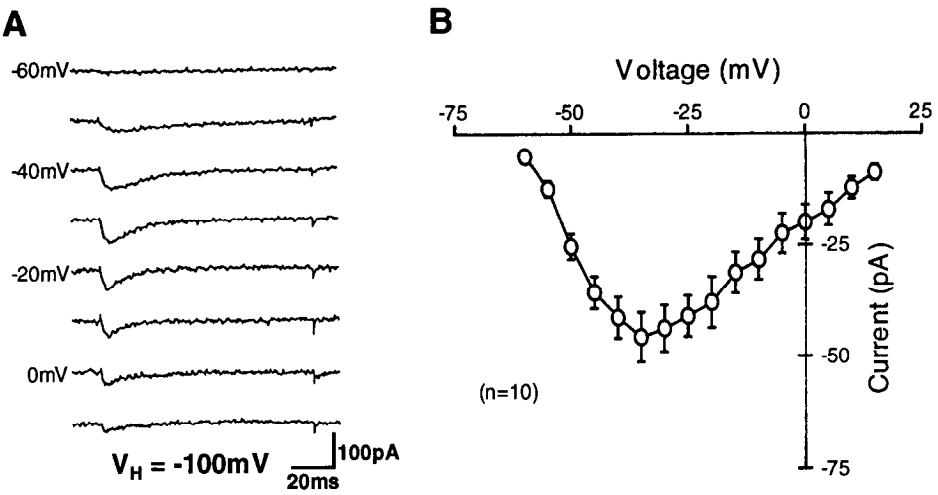

Figure 3. Current–voltage relationship of the isolated T current following blockade of HVA currents by intracellular fluoride. *A*, Records of isolated T current from a neuron at 10 hr in culture. Steps were from $V_H = -100$ mV to the indicated potentials. *B*, The *I–V* relation. Peak values of 50 pA are achieved by steps to −35 mV. Data are mean ± SEM of 10 cells.

and other divalent cations, as reported for calcium current in other systems (Kostyuk and Krishtal, 1977; Lux et al., 1990). Removal of both calcium and sodium then eliminated LVA current. Since many characteristics of this current including its pharmacological properties are similar to T current in other cells, as further shown below, we refer to this LVA current as T-type calcium current. The current exhibited little rundown during recordings of up to 30 min in duration.

HVA calcium current. HVA calcium current is activated at membrane potentials positive to −40 mV and is slowly inactivated (Barish, 1986, 1991a; O'Dowd et al., 1988). Two components were revealed by varying the holding potential. With $V_H = -100$ mV, the first component was activated at step potentials positive to −40 mV and threshold lay between −35 and −25 mV for most cells ($n > 200$; Fig. 1*A*). When V_H was changed from −100 mV to −50 mV, the slowly inactivating component disappeared and revealed a second, sustained component. Its threshold lay between −30 and −20 mV for most cells (Fig. 1*B*; $n > 100$). The slowly inactivating component is sensitive to holding potentials, similar to N-type HVA calcium current in other systems. The sustained component is insensitive to holding potential, similar to L-type HVA calcium current in other systems. Thus, with $V_H = -100$ mV, HVA current includes two components and makes a major contribution to the current observed with step potentials above −40 mV (Fig. 1*C*, open circles). Characterization of these components as N and L currents may not be useful, however, given the absence of consensus in regard to the criteria by which they should be identified. The current–voltage relationship with $V_H = -50$ mV displays only the sustained component at the same step potentials (Fig. 1*C*, squares). Subtraction of current recorded with $V_H = -50$ mV from current recorded with $V_H = -100$ mV yields LVA and a slowly inactivating HVA component (Fig. 1*C*, solid circles). The peaks for sustained, slowly inactivating and total HVA current all occur near 0 mV, with amplitudes of 252 ± 22 pA, 444 ± 43 pA, and 694 ± 10 pA, respectively ($n = 28$; Fig. 1*C*). Both components are eliminated by removal of extracellular calcium or addition of 2 mM $CoCl_2$ (Fig. 2, *bottom*).

The rates of inactivation for both HVA components are voltage dependent (Fig. 1*A*, bottom). When $V_H = -100$ mV and $V_S = 0$ mV, the time constant of inactivation was 63 ± 3 msec ($n = 17$), reflecting mainly the slowly inactivating component. When $V_H = -50$ mV and $V_S = 0$ mV, the sustained component had a time constant of inactivation of 158 ± 12 msec ($n = 17$). The two time constants are significantly different ($p < 0.05$). During recording, unlike LVA current, HVA current can run down rapidly in these neurons (O'Dowd et al., 1988). The rate of rundown was reduced from >50% to <20% during the first 15 min of recording when nucleotides were present in the pipette solution.

Physiological properties of T current

Current–voltage relationship. The T current of young and mature neurons can be isolated pharmacologically by blocking HVA current with fluoride (Kay et al., 1986; Kaneda et al., 1990; Fraser and MacVicar, 1991). T current is otherwise mixed with and further masked by HVA current at step potentials above −40 mV (Fig. 1*A*, *C*). For most cells ($n > 60$), internal application of fluoride via the recording pipette suppressed essentially all HVA calcium current with no apparent effect on T current (Fig. 3*A*). For some cells, a small residual HVA current persisted after this treatment. This current could be eliminated by subtracting the residual HVA current recorded at $V_H = -50$ mV from the current recorded at $V_H = -100$ mV.

The current–voltage relation of isolated T current reaches a maximum at a step potential near −35 mV with a mean amplitude of 46 ± 6 pA ($n = 10$) (Fig. 3*B*). The small size of the current introduces uncertainties that preclude accurate extrapolation of the reversal potential. With increased depolarization, the peak of the recorded current shifts to the left (Fig. 3*A*), indicating its increased rate of activation. In order to compare T current in cells of different size, the current density was calculated by normalizing peak amplitude recorded at −35 mV in each cell to its membrane surface area. The mean density of T current in mature neurons recorded in presence of fluoride was $2.0 \pm 0.2 \times 10^{-2}$ pA/μm² ($n = 10$). In roughly half of total cells recorded ($n > 200$), only T current was activated at step potentials of −35 mV. The density of T current in these cells, measured without application of fluoride, was $2.0 \pm 0.1 \times 10^{-2}$ pA/μm² ($n = 33$), and is not significantly different from that acquired in its presence ($p = 0.83$). To confirm further that fluoride does not alter T current, we also evaluated its effect on rates of activation and inactivation.

Rates of activation and inactivation. Both activation and inactivation of T current in young and mature neurons are voltage dependent and become faster with increased depolarization (Fig.

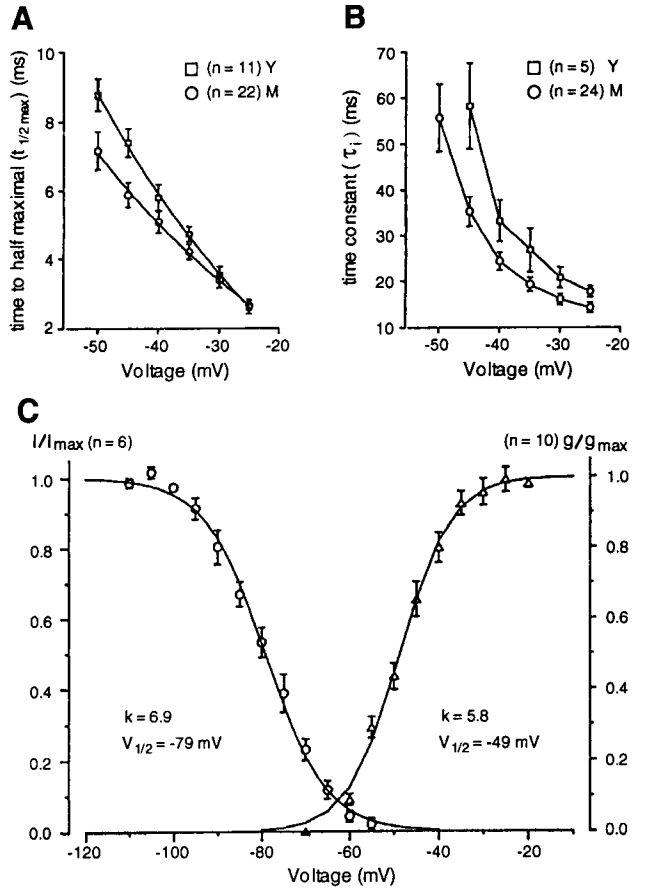

Figure 4. Activation and inactivation of T current. *A*, Activation rate in young and mature neurons (*squares* and *circles*, respectively) is represented by time to half-maximal current ($t_{1/2\,max}$). Data were fitted by a second-order regression curve. *B*, Inactivation rate in young and mature neurons (symbols as in *A*) is represented by the inactivation time constant (τ_i). The curve was generated by simple connection of the points. Activation and inactivation are voltage dependent and occur more rapidly with increased depolarization. For both young and mature neurons, experiments were performed on cells in which only T current was activated at a step potential of −35 mV; fluoride was not used to suppress HVA current. *C*, Activation and steady-state inactivation. *Right*, Activation is presented as percentage maximum conductance, calculated as the quotient of the current and the driving force. Data for analysis of activation of the T current were acquired from neurons analyzed in Figure 3. *Left*, Inactivation was evaluated by holding cells at various potentials for 30 sec, followed by steps to −35 mV. Fluoride treatment was omitted, since HVA currents are not activated at this test potential. Data from young and mature cells are calculated as percentage maximum current. Values for activation and steady-state inactivation are both fitted by Boltzmann relations (see text at right).

4*A*, *B*). The rate of activation of T current was measured as the time from stimulus onset to half-maximum current ($t_{1/2}$) at different step potentials. At −35 mV step potential, $t_{1/2}$ was 4.1 ± 0.2 msec (n = 12) for mature neurons using fluoride in the pipette solution. Time to half-maximum measured in cells lacking HVA current at this step potential was 4.2 ± 0.2 msec in the absence of fluoride (n = 22; Fig. 4*A*), demonstrating that it does not affect activation of T current (not significantly different; p = 0.66). Indeed, $t_{1/2}$ measured with or without fluoride was not significantly different at all step potentials from −55 to −25 mV. The rate of inactivation of the current was examined by fitting a single exponential to the inactivating part of the current after the peak. It was also voltage dependent (Fig. 4*B*). At −35 mV step potential, the time constant (τ_i) was 21 ± 1 msec (n = 14) in the presence of fluoride, and 19 ± 2 msec (n = 24) in its absence (p = 0.43).

Voltage-dependent activation and steady-state inactivation. Activation of T current at different membrane potentials was analyzed from data shown in the current–voltage relation (Fig. 3*B*). The amplitudes of T current at different potentials were transformed into conductances (G) according to the equation $G = I/(V - E_{Ca})$, where I is the current, V is the step potential, and E_{Ca} is the reversal potential for calcium current (estimated to be +45 mV based on data illustrated in Fig. 1*C*). Conductances were then normalized to the maximum conductance of T current, plotted as a function of step potential (Fig. 4*C*, right), and fitted by the Boltzmann relation

$$G/G_{max} = 1/\{1 + \exp[(V_{1/2} - V_S)/k]\},$$

where G is conductance at the step potential V_S, G_{max} is the maximum conductance, $V_{1/2}$ is the step potential yielding half-maximum conductance, and k is a steepness factor. The fit yields $V_{1/2}$ = −49 mV and k = 5.8 (Fig. 4*C*, right). Conductance is maximally activated at −25 mV.

Steady-state inactivation of T current was studied by systematically shifting the holding potential from −110 mV to −55 mV in 5 mV steps, for 30 sec each time, prior to steps to a test potential of −35 mV for 120 msec. The peak T current at different holding potentials was then normalized to the peak T current recorded from V_H = −110 mV to obtain the fraction of the current available at each holding potential (Fig. 4*C*, left). The steady-state inactivation of T current was fit with the Boltzmann relation

$$I/I_{max} = 1/\{1 + \exp[(V_H - V_{1/2})/k]\},$$

where I is the peak current at the holding potential V_H, I_{max} is the peak current from V_H = −110 mV, $V_{1/2}$ is the holding potential yielding half-inactivation of the current, and k is a steepness factor. $V_{1/2}$ of inactivation was −79 mV (k = 6.9). Inactivation is complete at −55 mV.

Pharmacological properties of T current

Effect of nickel on T current and HVA currents. We tested the effect of nickel on both T current and on HVA calcium currents of young and mature neurons, since it can block LVA T current specifically (Fox et al., 1987a; Narahashi et al., 1987; Hagiwara et al., 1988; Barish, 1991a; Mogul and Fox, 1991). When HVA current was eliminated with intracellular fluoride, superfusion with recording solution containing 50 μM nickel suppressed T current in all neurons (n > 20; Fig. 5*A*, (top), *C*). Similar results were obtained in the absence of fluoride, in cells lacking HVA current at step potentials more negative than −35 mV (n > 30). This low concentration of nickel had only a small effect on HVA calcium currents (Fig. 5*A*, bottom). However, higher concentrations of nickel (>50 μM) can reduce HVA current significantly as well; 200 μM nickel blocked ~40% of HVA current elicited by voltage steps from −100 to 0 mV (Fig. 6*A*). The effects of nickel on T current and HVA current were reversible after washout, although the extent of reversal was variable and complete recovery was rarely achieved. The dose–response relationships of the inhibitory effect of nickel on T current and HVA current are fit by sigmoid curves (Fig. 6*A*); T current was recorded in the presence of intracellular fluoride and HVA current was recorded in its absence. Half-maximal inhibition of T and HVA currents occurs at 13 ± 1 μM and 248 ± 1 μM, and the Hill

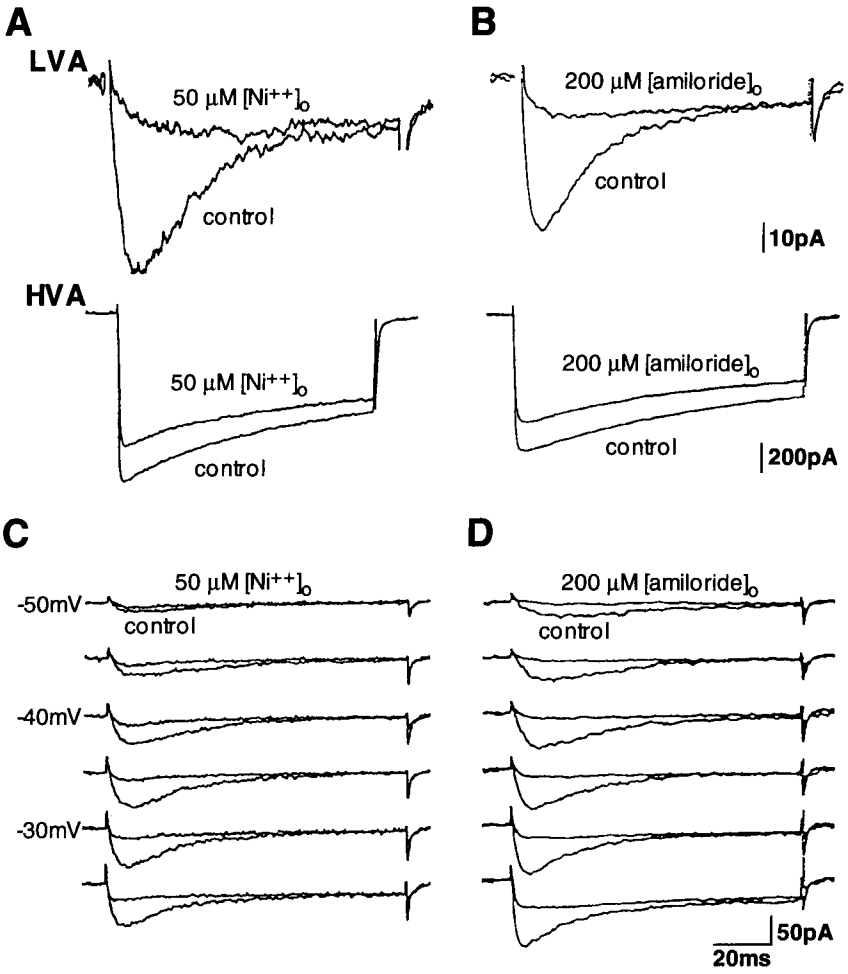

Figure 5. Pharmacological blockade of LVA (T) and HVA currents by nickel and amiloride. Agents were applied in the extracellular recording saline and block LVA current relatively specifically at the concentrations tested (*A*, *B*); 50 μM nickel and 200 μM amiloride both block most of the LVA current (*A* and *B*, *top*), but block less than 30% of HVA currents (*A* and *B*, *bottom*). Cells were held at −100 mV and stepped to −35 mV (*LVA*) or 0 mV (*HVA*). For both nickel (*C*) and amiloride (*D*), blockade of T current occurred at all step potentials from −50 to −25 mV with V_H = −100 mV. Records from one young (*C*) and three mature cells.

coefficients of these curves are 0.9 ± 0.1 (LVA) and 1.0 ± 0.1 (HVA), respectively. A single nickel ion may block a calcium channel for either the T or the HVA current in embryonic spinal neurons, since both Hill coefficients are close to 1. At a concentration of 50 μM, nickel blocks 75% of T current (Fig. 6*A*, arrow) but only 23% of HVA current. This concentration of nickel was used as a T current-specific blocker in later experiments.

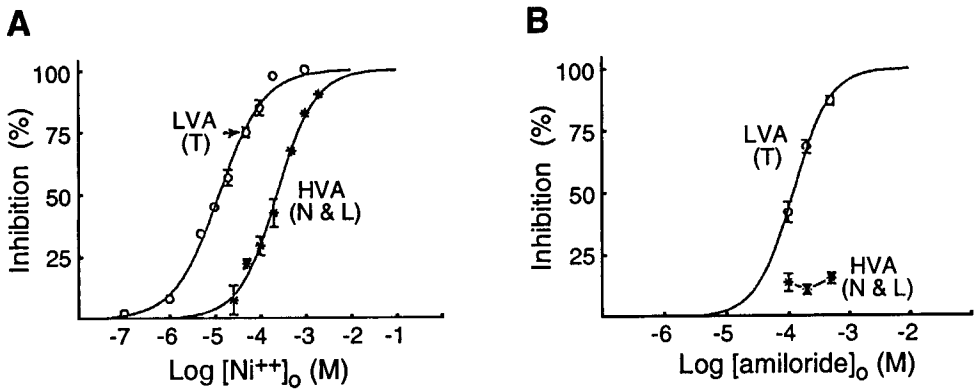

Figure 6. Dose–response curves for blockade of LVA (T) and HVA currents by nickel and amiloride. LVA currents were recorded in the presence of intracellular fluoride; HVA currents were recorded in its absence. Cells were held at V_H = −100 mV and stepped to −35 mV (*LVA*) or 0 mV (*HVA*). *A*, The percentage inhibition of Ca^{2+} currents is plotted as a function of log $[Ni^{2+}]_o$ (M). Each point is the mean of more than three cells (young and mature). SEM is indicated when greater than symbol size. Values for both LVA and HVA currents are fitted with sigmoid curves (○, *); 50% inhibition of LVA and HVA currents is obtained with 13 ± 1 μM and 248 ± 1 μM $[Ni^{2+}]$, respectively. Thus, LVA current is 20 times more sensitive to Ni^{2+} than HVA currents. Concentrations of Ni^{2+} less than 50 μM (*arrow*) affect mainly LVA current. Hill coefficients are 0.9 ± 0.1 (*LVA*) and 1.0 ± 0.1 (*HVA*). *B*, The percentage inhibition of calcium current is plotted as a function of log $[amiloride]_o$. Each point is the mean of >6 mature cells. Data for LVA current are fit with a sigmoid curve (○); 50% inhibition of LVA occurs at 124 ± 2 μM, and the Hill coefficient of the curve is 1.5. HVA currents are reduced by <20% at all concentrations tested (*).

Table 1. Developmental changes of calcium currents in cultured embryonic neurons

	Stage				
	Young (6–9 hr)	Middle (9–18 hr)	Mature (18–28 hr)	Mature (40–48 hr)	*t* test (*p* value)
Incidence of T current	87.0% (23)	80.7% (31)	67.0% (76)	35.3% (34)	
Density of T current (10^{-2} pA/μm^2)	1.79 ± .12 (21)	2.01 ± .13 (30)	2.02 ± .13 (33)	2.11 ± .19 (14)	$p \geq 0.14$
Density of HVA current (V_H = −100 mV) (10^{-2} pA/μm^2)	36.3 ± 1.6 (23)	ND	35.3 ± 1.6 (32)	32.3 ± 1.7 (31)	$p \geq 0.23$
Density of HVA current (V_H = −50 mV) (10^{-2} pA/μm^2)	13.1 ± 1.4 (12)	ND	12.4 ± 0.6 (20)	13.7 ± 0.9 (13)	$P \geq 0.12$

Data are the percentage of cells exhibiting T current decreases during development. About 60% of cells lose the T current during the first two d in culture. In contrast the current density in cells that express it does not change significantly during this period. Fluoride was not used in these experiments to block HVA current. The incidence and density of HVA current are constant during this time.

ND, no difference. Numbers in parentheses are number of neurons tested.

Effect of amiloride on T current and HVA currents. Amiloride, like nickel, has been reported to be a specific T current blocker in neurons and heart muscle cells (Tang et al., 1988; Tytgat et al., 1990; Mogul and Fox, 1991). We found that 100–500 μM amiloride could block T current and had only a small effect on HVA current in both young and mature neurons ($n > 40$). Addition of 200 μM amiloride to the recording solution eliminated most of the T current while HVA current was only slightly reduced (Fig. 5*B*, top and bottom). Furthermore, as with 50 μM nickel, blockade by amiloride occurred over the range of physiological potentials tested (Fig. 5*D*), as seen in heart muscle cells (Tytgat et al., 1990). Blockade of T current by amiloride was not affected by the presence or absence of fluoride in the pipette, and the effect of amiloride on T current was reversible after it was washed out. The dose–response relation for suppression of T current by amiloride is fit with a sigmoid curve (Fig. 6*B*). Half-maximal inhibition is achieved with 124 ± 2 μM and the Hill coefficient of the curve is 1.5. Two amiloride molecules may be required to block a single T current channel. With 100, 200, and 500 μM amiloride in the recording solution, HVA currents elicited with a step potential to 0 mV were reduced by 14 ± 4% ($n = 6$), 11 ± 2% ($n = 11$), and 15 ± 2% ($n = 3$), respectively. Amiloride at a concentration of 200–300 μM was used as a T current–specific blocker in later experiments.

Development of T and HVA currents in culture

T current is present in cultured cells as early as 6 hr after plating, during the calcium-sensitive period (Table 1). The threshold of T current lies between −60 and −50 mV in all neurons from 6 to 48 hr in culture. The current density is 1.8 ± 0.1 × 10^{-2} pA/μm^2 ($n = 21$) in 6–9 hr young neurons, 2.0 ± 0.1 × 10^{-2} pA/μm^2 ($n = 33$) in 18–24 hr mature neurons, and 2.1 ± 0.2 × 10^{-2} pA/μm^2 ($n = 14$) in 2-d-old neurons. There are no significant differences in density even at 2 d of age (for any pair, $p \geq 0.14$).

The rates of activation and inactivation of T current were also examined during development. Both the time to half-maximum activation and time constant of inactivation are slightly longer for T current in young neurons (Fig. 4). At a step potential of −35 mV, $t_{1/2}$ and τ_i from 6–9 hr neurons are 4.7 ± 0.2 msec ($n = 11$) and 27 ± 5 msec ($n = 5$), while values from 18–24 hr neurons are 4.2 ± 0.2 msec ($n = 22$) and 19 ± 2 msec ($n = 24$). The kinetics of activation and inactivation of the current in young and mature neurons are not significantly different ($p > 0.05$ for both $t_{1/2}$ and τ_i). No change in pharmacological susceptibility of the current was observed. The T current recorded in young neurons is sensitive to both nickel and amiloride at concentrations that block T current in mature cells.

Although the properties of the current remain the same, the incidence of T current in spinal neurons decreases markedly during development in culture (Table 1). T current was scored as absent when no current was detected at voltages below −45 mV. T current was recorded from 87% of young neurons, observed in 67% of mature neurons, and was found in 35% of cells at 2 d of age. The early appearance of T current and its subsequent disappearance at later stages of development have been described in other systems (Gonoi and Hasegawa, 1988; Kostyuk, 1989; McCobb et al., 1989; Thompson and Wong, 1989). These features suggest that T current may have a functional role in young neurons.

Developmental changes in HVA current were also studied. HVA current is present in all young and mature neurons. The density of HVA current does not change during first 2 d of development, confirming and extending previous observations (Table 1; O'Dowd et al., 1988). Furthermore, with holding potentials of −50 mV, the density of the relatively steady component of the current showed no significant change during this period. These results imply that the current density of the slowly inactivating component is also constant.

Function of T current in regulating intracellular calcium during early neuronal development

Characterization of changes in intracellular calcium in spontaneously active cells. Transient elevations of $[Ca^{2+}]_i$ monitored with fura-2 AM occur spontaneously in cultured neurons during the calcium-sensitive period (Holliday and Spitzer, 1990). Moreover, these calcium elevations require calcium influx through voltage-gated HVA channels. We have further characterized these calcium transients and examined the relationship between T current and spontaneous activity, to investigate the mechanisms by which T current regulates $[Ca^{2+}]_i$.

Spontaneous elevations of $[Ca^{2+}]_i$ were examined by a subtraction protocol to observe changes in indicator fluorescence occurring over short intervals. Cells at 6–9 hr in culture were loaded with the calcium-indicator dye fluo-3 AM. Images were accumulated during two successive periods of 100 sec each, and

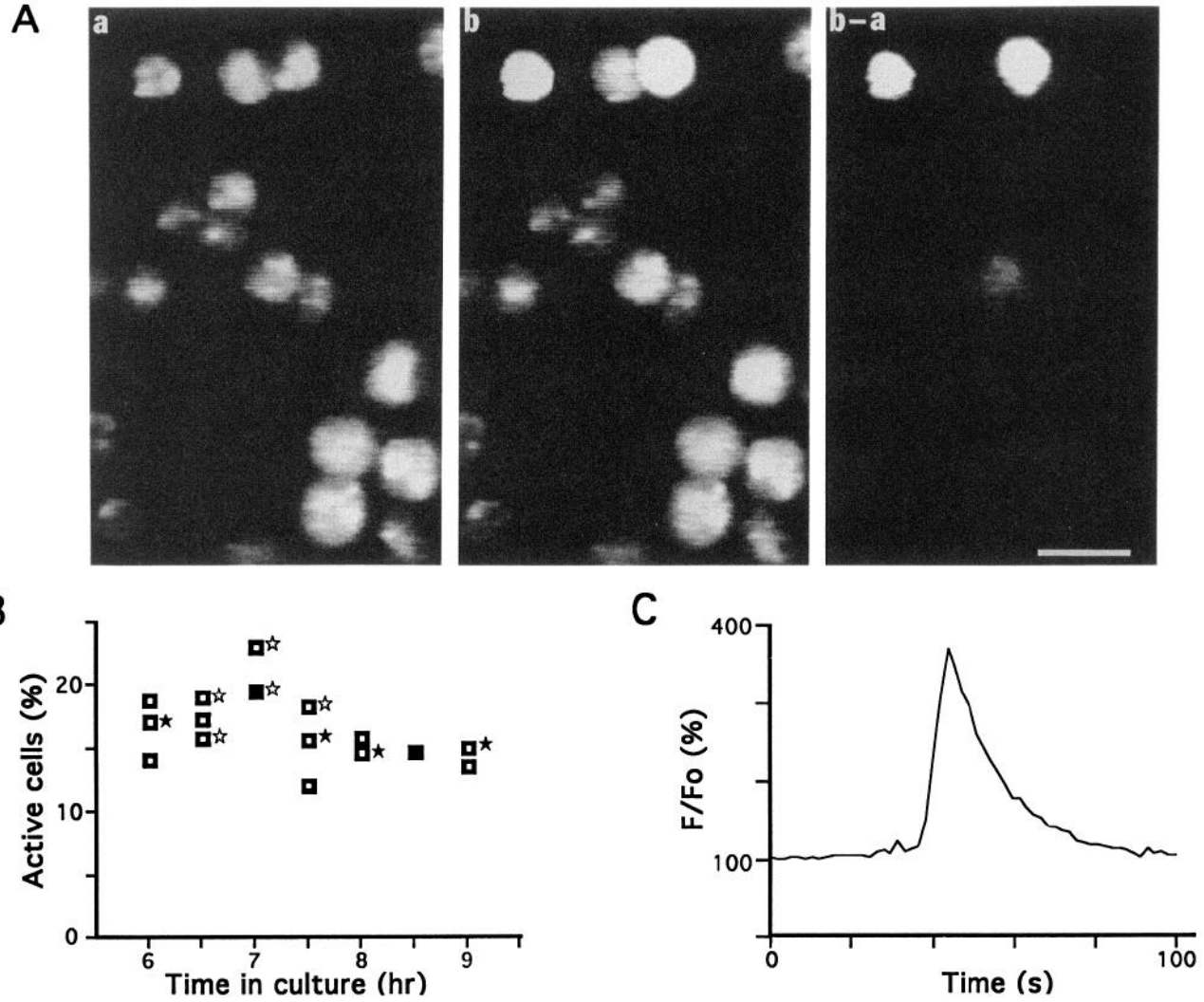

Figure 7. Analysis of spontaneous elevations of $[Ca^{2+}]_i$ by Ca^{2+} imaging with fluo-3 AM. *A*, The protocol for examination of "active" cells, exhibiting elevation of $[Ca^{2+}]_i$ during a 100 sec test period. Two fluorescent images of the same field of cells loaded with fluo-3 AM were accumulated during two consecutive 100 sec periods. The first (*a*) was used as a background image, subtracted from the second (*b*) to examine cells active during the test period. As shown in *b-a*, images of cells without elevation of $[Ca^{2+}]_i$ cancel each other out, and only those from cells active during the test period remain. This protocol was used to study factors regulating the change in $[Ca^{2+}]_i$. *B*, The percentage of active cells in control cultures during the 6–9 hr period after plating. *Open squares*, 10 mM Ca^{2+}; *solid squares*, 2 mM Ca^{2+}. Nickel (50 μM; *open stars*) or amiloride (200 μM; *solid stars*) were each applied to four of these cultures after control data were acquired. *C*, The time course of the change in fluorescence in an active cell. Image intensities were normalized to resting fluorescence, to reflect the elevation of intracellular calcium; image intensities were digitized at 3 sec intervals.

the first was digitally subtracted from the second (Fig. 7*A*). Several image fields were examined in each culture. "Active" cells were those that had spontaneous elevations of $[Ca^{2+}]_i$ during a 100 sec test period. They included neurons and undifferentiated cells and ranged from 12% to 23% of total cells examined (14 cultures; Fig. 7*B*). Cells not active during this period may have been active at earlier or later times. The highest percentage of active cells was seen around 7 hr after plating, consistent with previous studies (Holliday and Spitzer, 1990). To define the kinetics of transient increases in $[Ca^{2+}]_i$, the time course of changes in fluorescence was studied in 15 of these active cells (Fig. 7*C*). In 11, the increase achieved a maximum of 150–600% of the baseline level in less than 30 sec and decayed in less than 60 sec. The calcium elevation in these cells thus lasted for less than 90 sec. This increase is consistent with the sixfold increase in indicator fluorescence previously observed with application of a high concentration of potassium ions to stimulate young neurons (Holliday et al., 1991). A slower rise and decay of fluorescence were observed in the other four active cells, in which increases reached similar levels; the limited period of observation precluded definition of the time course of these changes.

A trigger mechanism is required for these "spontaneous" elevations of $[Ca^{2+}]_i$. HVA current promotes calcium influx and is necessary for spontaneous activity (Holliday and Spitzer, 1990), but its threshold lies positive to −40 mV (see also O'Dowd et al., 1988). Resting membrane potentials of these cells are below −90 mV in culture (0.67 mM KCl; Orida and Poo, 1978). Thus, substantial depolarization is necessary for activation of HVA current. Since T current has a lower threshold (−60 mV), it seemed possible that its activation depolarizes the membrane potential sufficiently to trigger activation of HVA current, lead-

Table 2. Blockade of T current alone is sufficient to suppress spontaneous elevations of $[Ca^{2+}]_i$

	Electrophysiological analyses			Functional analyses			
	$[Ca^{2+}]_o$ (mM)	% of control (peak current) LVA (T)	% of control (peak current) HVA (N & L)	No. of cells observed	No. of "active" cells (↑ $[Ca^{2+}]_i$)	% of "active" cells	Effect on (↑ $[Ca^{2+}]_i$)
Control	10	100	100	1197	208	17.4	—
Reducing $[Ca^{2+}]_o$	2	86[a]	78 ± 6	215	38	17.7	No
Adding 50 μM $[Ni^{2+}]_o$	10	25 ± 2	77 ± 2	676	39	5.8	Yes
Adding amiloride (200–300 μM)	10	31 ± 3	84 ± 3	577	30	5.2	Yes
Removing $[Ca^{2+}]_o$	0	0	0	216	7	3.2	Yes

[a] Estimated.

Young neurons were studied with the protocol illustrated in Figure 7. In controls, 17.4% of cells (8 cultures) were active. Reduction of $[Ca^{2+}]_o$ from 10 to 2 mM reduced LVA and HVA currents to 86% and 78% of controls, but had no effect on the percentage of active cells (two cultures). However, application of 50 μM $[Ni^{2+}]_o$ or 200–300 μM amiloride (four cultures for each), which reduces LVA and HVA currents to 25% and 77%, or 31% and 84% of control, respectively, suppressed the percentage of active cells. Since the difference between reduction in extracellular calcium and drug treatment lies in the percentage of LVA current remaining, this current is involved in triggering the increase in $[CA^{2+}]_i$.

ing to calcium influx and changes in $[Ca^{2+}]_i$. This hypothesis is supported by the following three lines of evidence.

Effects of nickel and amiloride on spontaneous elevations of intracellular calcium

To test the physiological role of T current in spontaneous elevations of $[Ca^{2+}]_i$ we used 50 μM nickel in calcium imaging experiments, since this concentration blocked most of the T current with relatively little effect on HVA currents. In controls, 208 cells among a total of 1197 in eight cultures exhibited spontaneous increases in $[Ca^{2+}]_i$ (17.4%; Table 2). After application of 50 μM nickel to four of these eight cultures (Fig. 7*B*, open stars), only 39 of 676 cells showed spontaneous activity (5.8%). Thus, specific blockade of T current with 50 μM nickel appears sufficient to inhibit spontaneous elevations of $[Ca^{2+}]_i$ in young neurons, even though most of the HVA calcium current remained unaffected.

To demonstrate further the role of T current in spontaneous elevations of $[Ca^{2+}]_i$, we also used amiloride in calcium imaging experiments. This agent specifically blocks T current in *Xenopus* embryonic spinal neurons. Among a total of 577 cells treated with 200–300 μM amiloride in four of these eight control cultures (Fig. 7*B*, solid stars), only 30 showed spontaneous activity (5.2%; Table 2). The result is consistent with the effects of application of 50 μM nickel, and reinforces the conclusion that T current is involved in spontaneous elevations of $[Ca^{2+}]_i$ in young neurons.

Additional experiments confirmed that the effects of 50 μM nickel and 200–300 μM amiloride are due to blockade of T current rather than HVA current, which is reduced by 25–31% (Table 2). Voltage-clamp recordings showed that reduction of external calcium from 10 mM to 2 mM blocked 22 ± 6% of HVA current, a reduction similar to that caused by 50 μM nickel or 200–300 μM amiloride. Spontaneous activity in cultures with 2 mM calcium was then examined. Of a total of 215 cells from two cultures (Fig. 7*B*, solid squares), 38 showed spontaneous activity (17.7%; Table 2). This percentage is not different from that seen in the presence of 10 mM calcium, and indicates that reduction of standard HVA current by nickel or amiloride does not affect spontaneous activity. This result is likely to be a consequence of the major contribution of intracellular free calcium by release from intracellular stores (Holliday et al., 1991), triggered by the remaining calcium influx. Addition of 50 μM nickel to one of these cultures grown in 2 mM calcium reduced the active cells to 4.4% (Fig. 7*B*). When extracellular calcium was omitted from the culture medium, only 3.2% of cells showed spontaneous activity (Table 2), consistent with previous findings (Holliday and Spitzer, 1990).

Selective blockade of T current by either nickel or amiloride suppresses spontaneous activity to an extent that is similar to that produced by the substantial blockade of HVA current with ω-conotoxin (5.8% and 5.2% vs 6%; Holliday and Spitzer, 1990). Since a similar effect can be produced by blockade of either T or HVA current, these two currents are likely to act in series to generate spontaneous elevations of $[Ca^{2+}]_i$ in these neurons. The observations support the hypothesis that T current depolarizes cells to trigger activation of HVA current, with calcium influx leading to release of calcium from intracellular stores and changes in $[Ca^{2+}]_i$.

Thresholds of inward currents. If T current initiates spontaneous activity by depolarizing cells and activating HVA current, it would be expected to have the lowest threshold among the known inward currents. Sodium current is also present in young neurons (O'Dowd et al., 1988). The threshold for sodium current activation was studied by equimolar replacement of 2 mM calcium with cobalt in normal recording solution, to eliminate all calcium currents. Sodium currents were activated between −45 and −35 mV in five young and five mature neurons. This result indicates that T current has lowest threshold (near −60 mV) among all inward currents and may act as a trigger.

Effects of T current on threshold of simulated action potentials

The effect of T current on the threshold of the action potential in young neurons was examined in computer simulations, with a model originally constructed to examine the function of HVA currents (Lockery and Spitzer, 1992). A threefold increase in amplitude and twofold increase in rate of activation of the delayed-rectifier potassium current account for most of the developmental change in action potential waveform. T current was fit using the standard Hodgkin-Huxley formulation for sodium current, replacing conductance with permeability and specifying driving force by the constant field equation. Satisfactory fits were obtained through the range of voltages at which the current is strongly activated (Fig. 8*A*; see Appendix for equations). Since this additional calcium current contributes to intracellular calcium dynamics that were driven by HVA currents in the previous model, the simulation of calcium-activated po-

tassium current (I_{Kc}) was also reevaluated (see Materials and Methods). I_{Kc} is both calcium and voltage dependent. As a result, the contribution of calcium by T current was sufficiently small in the voltage range of activation of I_{Kc} that its inclusion did not affect the modeling of this potassium current (Fig. 8*B*; compare to Fig. 8*C* of Lockery and Spitzer, 1992).

In contrast, the threshold of activation of the modeled young action potential was lowered by T calcium current. Since the model simulates action potentials recorded in 10 mM calcium, the voltages of activation of T current and I_{Kc} were shifted to more depolarized potentials, to compensate for the difference in surface charge under conditions of the recordings (2 and 0.1 mM calcium, respectively; see Materials and Methods). The action potential simulated without T current had a threshold of −21 mV; inclusion of T current lowered threshold to −36 mV (Fig. 8*C*). The effects of nickel and amiloride were also evaluated in the model. Reduction of T current to 25% or 31% (nickel and amiloride; Table 2) returned the threshold to −21 mV. In contrast, the threshold remained −36 mV following reduction of HVA current to 77% or 84%. Since the T current does not change its properties during the first day of development, the same equations were then used in modeling the contribution of this current to the action potential of mature neurons. Unlike the effect of this current in young cells, the T current has no impact on the threshold of mature neurons (Fig. 8*D*).

Discussion

Similarity of T currents in different systems

LVA T-type calcium current and its function during neuronal development in *Xenopus* spinal neurons were studied *in vitro* with whole-cell voltage-clamp and image analysis methods. We confirm that LVA calcium T current is present in *Xenopus* spinal neurons at 1 d in culture (Barish, 1991a), when the differentiation of electrical excitability is mature in many respects. The current in these embryonic spinal neurons is already present at earlier stages as well, and resembles that in other cells with a low threshold and rapid rate of activation and inactivation (Swandulla et al., 1991). T current was isolated by suppression of HVA current with fluoride, which has no effect on T current amplitude, voltage dependence, and rates of activation and inactivation. Maximum peak amplitudes of ~50 pA are recorded at a step potential of −35 mV. T currents seen in embryonic chick motoneurons, dorsal root ganglion cells, and ciliary ganglion neurons are also ~50 pA or less (Carbone and Lux, 1984; Gottmann et al., 1988; McCobb et al., 1989). In addition, the T current in *Xenopus* spinal neurons shares several other physiological and pharmacological properties with T current seen in other systems. The T current is half-activated at −49 mV and fully activated at −35 mV, and is half-inactivated at −79 mV and fully inactivated at −55 mV. The value of $V_{1/2}$ for activation is in good agreement with values of −45 to −55 mV seen in other systems (Fraser and MacVicar, 1991; O'Dell and Alger, 1991). The value for $V_{1/2}$ inactivation is similar to values of −70 to −85 mV seen by others (Coulter et al., 1989; Kaneda and Akaike, 1989; Kaneda et al., 1990; Fraser and MacVicar, 1991; O'Dell and Alger, 1991). These $V_{1/2}$ values are different from those reported by Barish (1991a; −49 mV vs −26 mV and −79 mV vs −52 mV), when recording from *Xenopus* spinal neurons cultured in a medium yielding more positive resting potentials.

Nickel and amiloride specifically block T current in neurons and muscle cells (Fox et al., 1987a; Hagiwara et al., 1988; Tang et al., 1988; Kaneda et at., 1990; Tytgat et al., 1990; Mogul and Fox, 1991) and block the T current in amphibian spinal neurons as well (Barish, 1991a). These agents were useful as blockers to determine the roles of T current in the generation of spontaneous elevations of $[Ca^{2+}]_i$. Both compounds could have nonspecific effects either on neurons or on the calcium indicator. However,

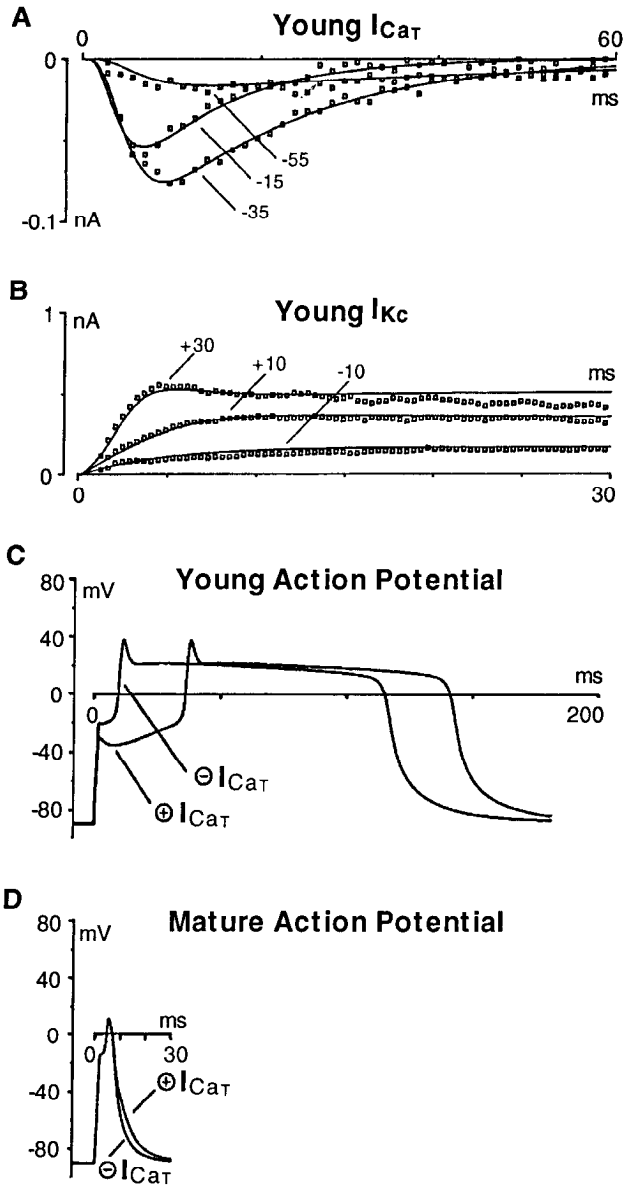

Figure 8. Simulation of currents and action potentials. *Squares*, recorded data; *lines*, simulated currents. *A*, T current recorded from a young neuron in 2 mM Ca^{2+}; data are plotted at 1.4 msec intervals. Holding potential, −100 mV. *B*, I_{Kc} recorded from a young neuron in 0.1 mM Ca^{2+}; data are plotted at 0.4 msec intervals. Holding potential, −90 mV (data from Lockery and Spitzer, 1992). Details of fitting procedures are provided in Materials and Methods. *C*, Action potentials in young neurons were elicited by 2 msec current pulses of 552 and 640 pA (±T current), from a holding potential of −90 mV. External concentration of calcium was 10 mM. Threshold is lowered from −21 to −36 mV by inclusion of this LVA calcium current. *D*, Action potentials in mature neurons were elicited by 2 msec current pulses of 697 and 698 pA (±T current), from a holding potential of −90 mV. Thresholds are −14 mV with and without the T current. See text at above left for details.

the similar effect of both agents on this current and on the spontaneous elevations of $[Ca^{2+}]_i$ suggests that the results are unlikely to be due to their nonspecific effects.

Changes in T current during development. The T current of embryonic *Xenopus* spinal neurons is present in young neurons during the calcium-sensitive period. Although there is no significant change in its properties, the current has been lost from more than half of mature neurons. This contrasts with HVA current, which persists in all neurons throughout this period (O'Dowd et al., 1988). Such early development of T current has also been seen in other embryonic systems, including rat hippocampal neurons (Yaari et al., 1987; Meyers and Barker, 1989), chick dorsal root ganglion cells and ciliary ganglion neurons (Gottmann et al., 1988), chick motoneurons (McCobb et al., 1989), rat hippocampal pyramidal neurons (Thompson and Wong, 1989), and neurons of the rat neostriatum (Bargas et al., 1991). During development the T current may decrease in amplitude or be completely lost (Beam and Knudson, 1988; Gonoi and Hasegawa, 1988; Kostyuk, 1989; McCobb et al., 1989). The early appearance of T current in different embryonic excitable cells suggests that it may play an important role in their development.

The development of the T current has also been studied *in vivo* in *Xenopus* embryos (Desarmenien et al., 1993). The increase in rate of activation seen *in vitro* is slightly more rapid *in vivo*. In addition, the current density shows an initial increase *in vivo* that does not occur in culture. It is possible that factors necessary for this increase are removed when cells are isolated *in vitro*.

Function of the T current. The function of T current in neuronal development is a major issue addressed in this study. In mature neurons and heart muscle cells, T current plays a role in regulating the firing rate (Hagiwara et al., 1988; Lovinger and White, 1989; Suzuki and Rogawski, 1989; White et al., 1989; Leresche et al., 1990; Pirchio et al., 1990; Soltesz et al., 1991; Huguenard and Prince, 1992). Its function in embryonic neurons during development has been largely unknown. We find that T current is not only present during the period when cultured *Xenopus* spinal neurons are sensitive to external calcium but is also directly involved in spontaneous elevations of $[Ca^{2+}]_i$ that regulate their differentiation.

The mechanism by which T current regulates $[Ca^{2+}]_i$ is likely to be its depolarization of the membrane potential to activate HVA current and promote the elevation of $[Ca^{2+}]_i$. Experimental evidence supporting this hypothesis is provided by the results of application of 50 μM nickel or 200–300 μM amiloride, both of which suppress of spontaneous elevations of $[Ca^{2+}]_i$ in young neurons. These results indicate that blockade of T current alone can block increases $[Ca^{2+}]_i$. Moreover, since blockade of either T or HVA current has the same effect on spontaneous activity, these two currents are likely to interact in series to increase $[Ca^{2+}]_i$ as proposed.

Several properties of these neurons support the role of T current in triggering activation of HVA current in young neurons. First, the timing of expression of T current is appropriate, since it is present in all young neurons during the calcium-sensitive period. Second, the T current has the lowest threshold among all known inward currents in young neurons, and is the first to be activated upon depolarization. Third, opposing outward potassium currents are smaller (Barish, 1986; O'Dowd et al., 1988) and the input resistance is larger (~2 GΩ) in young neurons than in mature cells, probably because there are fewer ion channels at this stage of development (Baccaglini and Spitzer, 1977; Blair, 1983; O'Dowd, 1983; Harris et al., 1988). Thus, the relatively small T current is more likely to achieve sufficient depolarization to bring the membrane potential to threshold for sodium and HVA calcium currents. Moreover, the ensuing depolarization may initiate an action potential, since activation of HVA current in young neurons can produce calcium-dependent action potentials. This conclusion is supported by the results of computer simulations, which show that the presence of T current lowers the threshold of the action potential of young neurons. However, T current has no effect on the threshold of mature neurons in computer simulations and spontaneous elevations of $[Ca^{2+}]_i$ in mature neurons are decreased. This suggests that its function in eliciting action potentials is restricted to young neurons, as a consequence of increases in potassium current density that occur gradually during their maturation (O'Dowd et al., 1988). Sustained subthreshold depolarizations have been proposed to account for the elevation of $[Ca^{2+}]_i$ in mature neurons (Barish, 1991b); however, role of such elevations of $[Ca^{2+}]_i$ in affecting neuronal development is unclear.

Image analysis of spontaneous changes in intracellular calcium in cultured neurons. Changes in levels of $[Ca^{2+}]_i$ in young neurons were examined with the calcium-dependent fluorescent dye fluo-3 AM. Spontaneous elevations of fluorescence, reflecting changes in $[Ca^{2+}]_i$, were seen in cultured cells at 6–9 hr *in vitro*, as previously reported (Holliday and Spitzer, 1990). Many active cells are neurons, although some are morphologically undifferentiated cells that may become neurons later. The transient nature of the rapid increase of $[Ca^{2+}]_i$ was identified in these spontaneously active cells. In addition, the peak of the wave of indicator fluorescence was sixfold above baseline, similar to results obtained by depolarization of neurons with high potassium to mimic action potentials (Holliday et al., 1991). These findings suggest that elevations of $[Ca^{2+}]_i$ may be associated with spontaneous action potentials in young neurons.

Reduction of extracellular calcium from 10 to 2 mM caused no diminution of spontaneous activity, although HVA current was reduced by 78%. However most of the change in $[Ca^{2+}]_i$ detected in depolarized cells is contributed by calcium-induced calcium release from intracellular stores (Holliday et al., 1991). LVA current is largely spared by the reduction of external calcium, and its summation with the large remaining HVA current is likely to be sufficient to act as trigger for this calcium release.

While LVA current appears to be the trigger for activation of HVA current in young neurons, the trigger for activation of T current remains to be determined. The cues for depolarization could be extracellular, such as growth factors, neurotransmitters, or substrate adhesion molecules. Alternatively, the cues could be intracellular, and involve normal metabolites. This possibility is favored by the observation that single cells differentiate in isolation in a fully defined medium much as they do *in vivo* (Henderson and Spitzer, 1986), with respect to excitability, neurotransmitter sensitivity, and neurite elongation. Metabolic control of excitability is particularly well studied in pancreatic β-cells (Ashcroft and Rorsman, 1989; Peterson, 1992). Similar mechanisms may control spontaneous activity of amphibian spinal neurons, since embryonic cells exhibit high levels of metabolic activity at early stages of development.

Appendix

Young I_{CaT}

$$I_{CaT} = f_{Ca}\bar{P}_{Ca}A_{Ca}^{5}B_{Ca}\mathcal{E}_{Ca},$$

where f_{Ca} is a scale factor converting the amplitude of the exemplar to the mean current size, $\bar{P}_{Ca}$ is the membrane permeability to calcium, A_{Ca} and B_{Ca} are expressions for steady-state activation and inactivation, and E_{Ca} is the driving force given by the constant field equation. $\tau_{A,Ca}$ and $\tau_{B,Ca}$ are the time constants of activation and inactivation, respectively.

$$f_{Ca} = 0.26,$$

$$\bar{P}_{Ca} = 0.21,$$

$$A_{Ca,\infty}(V) = \frac{1}{1 + e^{(58.6+V)/-9.7}},$$

$$B_{Ca,\infty}(V) = \frac{1}{1 + e^{(79+V)/6.9}},$$

$$E_{Ca} = \frac{15300(-[Ca]_o)V}{e^{0.8V} - 1},$$

$$\tau_{A,Ca} = 20.2\left(\frac{1 - 0.06}{1 + e^{(141+V)/42}} + 0.06\right),$$

$$\tau_{B,Ca} = 300\left(\frac{1 - 0.03}{1 + e^{(80.16+V)/12.7}} + 0.03\right).$$

References

Alonso MT, Sanchez A, Garcia-Sancho J (1990) Arachidonic acid-induced calcium influx in human platelets. Biochem J 272:435–443.

Baccaglini PI, Spitzer NC (1977) Developmental changes in the inward current of the action potential of Rohon-Beard neurones. J Physiol (Lond) 271:93–117.

Bargas J, Surmeier DJ, Kitai ST (1991) High- and low-voltage activated calcium currents are expressed by neurons cultured from embryonic rat neostriatum. Brain Res 541:70–74.

Barish ME (1986) Differentiation of voltage-gated potassium current and modulation of excitability in cultured embryonic *Xenopus* spinal neurones. J Physiol (Lond) 375:229–250.

Barish ME (1991a) Voltage-gated calcium currents in cultured embryonic *Xenopus* spinal neurones. J Physiol (Lond) 444:523–543.

Barish ME (1991b) Increases in intracellular calcium ion concentration during depolarization of cultured embryonic *Xenopus* spinal neurones. J Physiol (Lond) 444:545–565.

Beam BP (1989) Classes of calcium channels in vertebrate cells. Annu Rev Physiol 51:367–384.

Beam KG, Knudson CM (1988) Calcium currents in embryonic and neonatal mammalian skeletal muscle. J Gen Physiol 91:781–798.

Bixby JL, Spitzer NC (1984) Early differentiation of vertebrate spinal neurons in the absence of voltage-dependent Ca^{++} and Na^{+} influx. Dev Biol 106:89–96.

Blair LAC (1983) The timing of protein synthesis required for the development of the sodium action potential in embryonic spinal neurons. J Neurosci 3:1430–1436.

Carbone E, Lux HD (1984) A low voltage-activated calcium conductance in embryonic chicken sensory neurons. Biophys J 46:413–418.

Coulter DA, Huguenard JR, Prince DA (1989) Calcium currents in rat thalamocortical relay neurones: kinetic properties of the transient, low-threshold current. J Physiol (Lond) 414:587–604.

Desarmenien MG, Spitzer NC (1991) Role of calcium and protein kinase C in development of the delayed rectifier potassium current in *Xenopus* spinal neurons. Neuron 7:797–805.

Desarmenien MG, Clendening B, Spitzer NC (1993) *In vivo* development of voltage-dependent ionic currents in *Xenopus* embryonic spinal neurons. J Neurosci 13:2575–2581.

Fox AP, Nowycky MC, Tsien RW (1987a) Kinetic and pharmacological properties distinguishing three types of calcium currents in chick sensory neurones. J Physiol (Lond) 394:149–172.

Fox AP, Nowycky MC, Tsien RW (1987b) Single-channel recordings of three types of calcium channels in chick sensory neurones. J Physiol (Lond) 394:173–200.

Fraser DD, MacVicar BA (1991) Low-threshold transient calcium current in rat hippocampal lacunosum-moleculare interneurons: kinetics and modulation by neurotransmitters. J Neurosci 11:2812–2820.

Gonoi T, Hasegawa S (1988) Post-natal disappearance of transient calcium channels in mouse skeletal muscle: effects of denervation and culture. J Physiol (Lond) 401:617–637.

Gottmann K, Dietzel ID, Lux HD, Huck S, Rohrer H (1988) Development of inward currents in chick sensory and autonomic neuronal precursor cells in culture. J Neurosci 8:3722–3732.

Gu X, Spitzer NC (1991) T-type Ca^{++} current and its function in triggering Ca^{++} influx in embryonic *Xenopus* spinal neurons. Soc Neurosci Abstr 17:1159.

Hagiwara N, Irisawa H, Kameyama M (1988) Contribution of two type of calcium currents to the pacemaker potentials of rabbit sino-atrial node cells. J Physiol (Lond) 395:233–253.

Hamill OP, Marty A, Neher E, Sakmann B, Sigworth FG (1981) Improved patch-clamp techniques for high resolution current recording from cells and cell-free membrane patches. Pfluegers Arch 391:85–100.

Harris GL, Henderson LP, Spitzer NC (1988) Changes in densities and kinetics of delayed rectifier potassium channels during neuronal differentiation. Neuron 1:739–750.

Henderson LP, Spitzer NC (1986) Autonomous early differentiation of neurons and muscle cells in single cell cultures. Dev Biol 113:381–387.

Henderson LP, Smith MA, Spitzer NC (1984) The absence of calcium blocks impulse-evoked release of acetylcholine but not *de novo* formation of functional neuromuscular synaptic contacts in culture. J Neurosci 4:3140–3150.

Hess P (1990) Calcium channels in vertebrate cells. Annu Rev Neurosci 13:337–356.

Holliday J, Spitzer NC (1990) Spontaneous calcium influx and its roles in differentiation of spinal neurons in culture. Dev Biol 141:13–23.

Holliday J, Adams RJ, Sejnowski TJ, Spitzer NC (1991) Calcium-induced release of calcium regulates differentiation of cultured spinal neurons. Neuron 7:787–796.

Huguenard JR, Prince DA (1992) A novel T-type current underlies prolonged Ca^{2+}-dependent burst firing in GABAergic neurons of rat thalamic reticular nucleus. J Neurosci 12:3804–3817.

Hussy N (1991) Developmental change in calcium-activated chloride current during the differentiation of *Xenopus* spinal neurons in culture. Dev Biol 147:225–238.

Kaneda M, Akaike N (1989) The low-threshold Ca current in isolated amygdaloid neurons in the rat. Brain Res 497:187–190.

Kaneda M, Wakamori M, Ito C, Akaike N (1990) Low-threshold calcium current in isolated Purkinje cell bodies of rat cerebellum. J Neurophysiol 63:1046–1051.

Kay AR, Miles R, Wong RKS (1986) Intracellular fluoride alters the kinetic properties of calcium currents facilitating the investigation of synaptic events in hippocampal neurons. J Neurosci 6:2915–2920.

Kostyuk PG (1989) Diversity of calcium ion channels in cellular membranes. Neuroscience 28:253–261.

Kostyuk PG, Krishtal OA (1977) Effects of calcium and calcium-chelating agents on the inward and outward current in the membrane of mollusc neurones. J Physiol (Lond) 270:569–580.

Kostyuk PG, Shuba Y, Savchenko AN (1988) Three types of calcium channels in the membrane of mouse sensory neurons. Pfluegers Arch 411:661–669.

Leresche N, Jassik-Gerschenfeld D, Haby M, Soltesz I, Crunelli V (1990) Pacemaker-like and other types of spontaneous membrane potential oscillations of thalamocortical cells. Neurosci Lett 113:72–77.

Lipscombe D, Madison DV, Poenie M, Reuter H, Tsien RW, Tsien RY (1988) Imaging of cytosolic Ca^{2+} transients arising from Ca^{2+} stores and Ca^{2+} channels in sympathetic neurons. Neuron 1:355–365.

Lockery SR, Spitzer NC (1992) Reconstruction of action potential development from whole-cell currents of differentiating spinal neurons. J Neurosci 12:2268–2287.

Lovinger DM, White G (1989) Post-natal development of burst firing behavior and the low-threshold transient calcium current examined using freshly isolated neurons from rat dorsal root ganglia. Neurosci Lett 102:50–57.

Lux HD, Carbone E, Zucker H (1990) Na^{+} currents through low-

voltage-activated Ca^{2+} channels of chick sensory neurones: block by external Ca^{2+} and Mg^{2+}. J Physiol (Lond) 430:159–188.
McCobb DP, Best PM, Beam KG (1989) Development alters the expression of calcium currents in chick limb motoneurons. Neuron 2:1633–1643.
Meyer T, Stryer L (1991) Calcium spiking. Annu Rev Biophys Biophys Chem 20:53–174.
Meyers DE, Barker JL (1989) Whole-cell patch-clamp analysis of voltage-dependent calcium conductances in cultured embryonic rat hippocampal neurons. J Neurophysiol 61:467–477.
Minta A, Kao JPY, Tsien RY (1989) Fluorescent indicators for cytosolic calcium based on rhodamine and fluorescein chromophores. J Biol Chem 264:8171–8178.
Mogul DJ, Fox AP (1991) Evidence for multiple types of Ca^{2+} channels in acutely isolated hippocampal CA3 neurones of the guinea-pig. J Physiol (Lond) 433:259–281.
Murray RK, Kotlikoff MI (1991) Receptor-activated calcium influx in human airway smooth muscle cells. J Physiol (Lond) 435:123–144.
Narahashi T, Tsunoo A, Yoshii M (1987) Characterization of two types of calcium channels in mouse neuroblastoma cells. J Physiol (Lond) 383:231–249.
Nieuwkoop JM, Faber J (1967) Normal table of *Xenopus laevis* (Daudin): a systematic and chronological survey of the development of the fertilized egg till the end of metamorphosis, 2d ed. Amsterdam: North-Holland.
O'Dell TJ, Alger BE (1991) Single calcium channels in rat and guinea-pig hippocampal neurones. J Physiol (Lond) 436:739–767.
O'Dowd DK (1983) RNA synthesis dependence of action potential development in spinal cord neurones. Nature 303:619–621.
O'Dowd DK, Ribera AB, Spitzer NC (1988) Development of voltage-dependent calcium, sodium, and potassium currents in *Xenopus* spinal neurons. J Neurosci 8:792–805.
Orida N, Poo M (1978) Electrophoretic movement and localization of acetylcholine receptors in embryonic muscle cell membrane. Nature 275:31–35.
Pirchio M, Lightowler S, Crunelli V (1990) Postnatal development of the T calcium current in cat thalamocortical cells. Neuroscience 38: 39–45.
Reber BFX, Reuter H (1991) Dependence of cytosolic calcium in differentiating rat pheochromocytoma cells on calcium channels and intracellular stores. J Physiol (Lond) 435:145–162.
Ribera AB, Spitzer NC (1989) A critical period of transcription required for differentiation of the action potential of spinal neurons. Neuron 2:1055–1062.
Ribera AB, Spitzer NC (1990) Differentiation of I_{KA} in amphibian spinal neurons. J Neurosci 10:1886–1891.
Soltesz I, Lightowler S, Leresche N, Jassik-Gerschenfeld D, Pollard CE, Crunelli V (1991) Two inward currents and the transformation of low-frequency oscillations of rat and cat thalamocortical cells. J Physiol (Lond) 441:175–197.
Spitzer NC, Lamborghini JE (1976) The development of the action potential mechanism of amphibian neurons isolated in cell culture. Proc Natl Acad Sci USA 73:1641–1645.
Spitzer NC, de Baca RC, Allen KA, Holliday J (1993) Calcium dependence of differentiation of GABA immunoreactivity in spinal neurons. J Comp Neurol, in press.
Suzuki S, Rogawski MA (1989) T-Type calcium channels mediate the transition between tonic and phasic firing in thalamic neurons. Proc Natl Acad Sci USA 86:7228–7232.
Swandulla D, Carbone E, Lux HD (1991) Do calcium channel classifications account for neuronal calcium channel diversity? Trends Neurosci 14:46–51.
Tang CM, Presser F, Morad M (1988) Amiloride selectively blocks the low threshold (T) calcium channel. Science 240:213–215.
Thompson SM, Wong RKS (1989) Low threshold, transient calcium current is present in young, but not adult, isolated rat hippocampal pyramidal cells. Soc Neurosci Abstr 15:653.
Tsien RW, Tsien RY (1990) Calcium channels, stores, and oscillations. Annu Rev Cell Biol 6:715–760.
Tsien RW, Fox AP, Hess P, McCleskey EW, Nilius B, Nowycky MC, Rosenberg RL (1987) Multiple types of calcium channel in excitable cells. Soc Gen Physiol Ser 41:167–187.
Tsien RW, Lipscombe D, Madison DV, Bley KR, Fox AP (1988) Multiple types of neuronal calcium channels and their selective modulation. Trends Neurosci 11:431–438.
Tytgat J, Vereecke J, Carmeliet E (1990) Mechanism of cardiac T-type Ca^{2+} channel blockade by amiloride. J Pharmacol Exp Ther 254:546–551.
White G, Lovinger DM, Weight FF (1989) Transient low-threshold Ca^{2+} current triggers burst firing through an afterdepolarizing potential in an adult mammalian neuron. Proc Natl Acad Sci USA 86: 6802–6806.
Yaari Y, Hamon B, Lux HD (1987) Development of two types of calcium channels in cultured mammalian hippocampal neurons. Science 235:680–682.